

Solid-state effects on nonradiative decay of $4d^9 4f^1$ states in barium halides

Masao Kamada

Institute for Molecular Science, Myodaiji, Okazaki, Aichi 444, Japan

Kouichi Ichikawa and Osamu Aita

College of Engineering, University of Osaka Prefecture, Mozu, Sakai, Osaka 591, Japan

(Received 14 July 1992; revised manuscript received 29 September 1992)

The nonradiative decay of $4d^9 4f^1$ states in barium halides was investigated by using resonant-photoemission spectroscopy. Constant-final-state spectra with the final state at $N_{4,5}-O_{2,3}O_{2,3}$ Auger electron peak and constant-initial-state (CIS) spectra with the initial state at Ba $5p$ levels were enhanced in the Ba $4d$ excitation-energy region, indicating Auger and direct recombination decay processes, respectively. The probability of the direct recombination decay was estimated from the CIS and the absorption spectra. At the excitation energy of the $4d^9 4f^1$ (3D) state, the intensity ratio of $5p_{1/2}$ to $5p_{3/2}$ photoelectrons showed the anomalous increase due to the different branching ratio in the direct recombination process. It was noticed that the decay probability through the direct recombination process and the degree of the anomalous branching ratio increase in the order of BaF_2 , $BaCl_2$, and $BaBr_2$. This result indicates that the nonradiative decay of the $4d^9 4f^1$ states in the barium halides is affected by crystalline environments.

I. INTRODUCTION

The localization or delocalization of $4f$ electrons is of much interest, because $4f$ electrons are closely related to a variety of electrical and magnetic properties of rare-earth compounds. There have been many studies to understand the relation between them.¹ On the other hand, $4f$ electrons in the core excitation have attracted recent interest because they also show a variety of localization or delocalization behaviors. Through the years, there have been many studies on the absorption spectra of atoms or ions with $Z=54-70$ in the region of $4d \rightarrow nf, \epsilon f$ excitations ($n=4, 5$, and so on, and ϵ is the continuum states).²⁻¹³ The absorption spectra are characterized by huge peaks and weak sharp lines. The latter is due to the multiplet structures of $4d^9 4f^{m+1}$ states (m is the number of $4f$ electrons in the ground state), while the former depends on the potential barrier separating inner and outer wells for $4f$ electrons. The inner well becomes narrower and deeper with increasing nuclear charge Z and then leads to the sudden collapse of the $4f$ wave functions from the outer into the inner well. The strong absorption peaks are interpreted in terms of delayed onsets of $4d \rightarrow \epsilon f$ transitions for lighter elements [$Z \leq 54$ (Xe)], while for heavier elements [$Z \geq 56$ (Ba)] the observed absorption peaks arise from the $4d^9 4f^{m+1}$ states autoionized in the continuum.

However, these explanations of the observed spectra are not fully satisfactory. Jo¹³ has demonstrated the effect of valence mixing on multiplet structures in the Ce $4d$ photoabsorption spectra for Ce compounds, on the basis of the impurity Anderson model. He showed the deviation of the spectra for CeO_2 from the multiplet structure with integral valence, and attributed it to a strong interference between the $4d^{10} 4f^0 \rightarrow 4d^9 4f^1$ and

$4d^{10} 4f^1 \nu \rightarrow 4d^9 4f^2 \nu$ photoexcitations (ν refers to a hole in the valence state). Miyahara *et al.*¹⁰ have measured the $4d$ photoabsorption spectra of La, LaF_3 , Ba, and BaF_2 , and found the difference of the absorption structures between metallic Ba and BaF_2 , and between the amorphous and crystalline BaF_2 . They have suggested that the amount of hybridization of $5f$ or $6f$ states with a $4d^9 4f^1$ (1P) state or continuum states is independent on the crystal structure. These results indicate that the decay process of $4d^9 4f^{m+1}$ states is not completely interpretable within an atomic picture.

Recently we^{14,15} have investigated decay processes of $4d$ excited states in Cs halides and BaF_2 and LaF_3 by means of resonant photoemission spectroscopy, and found that their $4d$ excited states decay dominantly through the $N_{4,5}-O_{2,3}O_{2,3}$ Auger process, where $N_{4,5}$ denotes the initial N_4 or N_5 hole and $O_{2,3}$ denotes the final O_2 or O_3 hole state, and that the localization of the $4d$ excited states is not constant over the $4d$ excitation region. The purpose of the present study is to examine the decay process of the $4d^9 4f^1$ excited states in Ba halides in more detail, because they have no $4f$ electrons in the ground state, but have a $4f$ electron with a $4d$ hole in the excited state as Cs, La, and some Ce compounds.

II. EXPERIMENTAL PROCEDURES

Photoelectron experiments were carried out by using synchrotron radiation from an electron storage ring at the Institute for Solid State Physics of the University of Tokyo. The spectral band width of a 2-m grazing-incidence monochromator was about 0.18 eV at the photon energy of 90 eV, and the electron-analyzer resolution was constant with a full width at half maximum (FWHM) of 0.4 eV. Barium halides were prepared *in situ* by eva-

poration onto gold substrates. The absorption measurements were performed by using synchrotron radiation from a 750-MeV storage ring (UVSOR) at the Institute for Molecular Science. A 2-m Grasshopper monochromator was used for the present measurement. The spectral width was set to be the same as that of the monochromator used for the measurement of the photoelectron spectra. The other experimental procedures have been described in detail in Refs. 14 and 15.

III. EXPERIMENTAL RESULTS

Figures 1 and 2 show sets of photoelectron spectra of BaCl_2 and BaBr_2 , respectively, which were obtained with various photon energies around the Ba $4d$ threshold. The photon energy of 90.5 eV and 94.2 or 94.3 eV corresponds to the excitation energy of the 3P and 3D multiplet states ($4d^9 4f^1$), respectively, while the other photon energies are shown with an equal distance in energy. The binding energies are given relative to the top of the valence band. The ordinate is proportional to the number of photoelectrons per unit incident photon flux. The spectral distribution of incident photon flux was determined from a photoelectric yield spectrum of gold. The valence-band spectrum of BaCl_2 shows a single peak, while that of BaBr_2 consists of a peak and a shoulder on its higher binding-energy side. Two components observed in the valence spectrum of BaBr_2 are attributed to the spin-orbit splitting of Br $4p$ orbitals. The outermost s level of the halogen was appreciable between the Ba $5p_{1/2}$

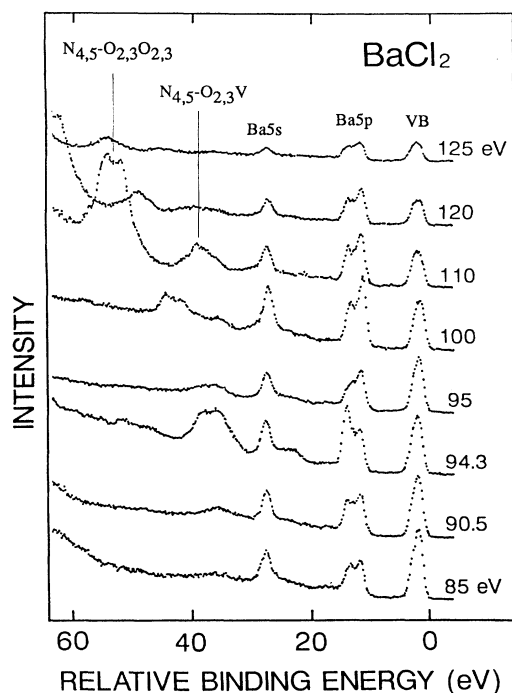


FIG. 1. A set of the photoelectron spectra of BaCl_2 obtained with various photon energies around the Ba $4d$ excitation energy. The binding energy is given relative to the top of the valence band. The intensities are normalized to the incident photon flux.

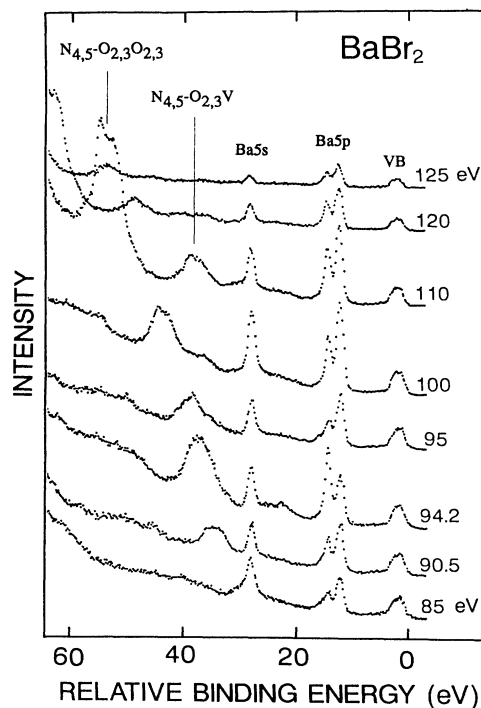


FIG. 2. A set of the photoelectron spectra of BaBr_2 obtained with various photon energies around the Ba $4d$ excitation energy. The binding energy is given relative to the top of the valence band. The intensities are normalized to the incident photon flux.

and Ba $5p_{3/2}$ spectra in BaCl_2 , but could not be clearly observed in BaBr_2 . By taking account of the binding energy, it is supposed that the Br $4s$ level is buried in the tail of the Ba $5p_{3/2}$ spectrum in BaBr_2 . The binding energies of the valence band and the inner-core levels in the energy-distribution curves are listed in Table I (see Fig. 2 and Table I in Ref. 15 for BaF_2).

The $N_{4,5}\text{-O}_{2,3}$ and $N_{4,5}\text{-O}_{2,3}\text{V}$ Auger electron peaks are observed when the excitation-photon energy is beyond 90 eV. Kinetic energies of the Auger electron peaks, which

TABLE I. The binding energies of valence-band and inner-core levels, as well as the kinetic energies of Auger electrons observed at 110 eV. Energies are relative to the top of the valence band and are given in electron volts.

	BaCl_2	BaBr_2
Valence band	2.0	1.2/2.4
Ba $5p_{3/2}$	11.4	12.2
$5p_{1/2}$	13.6	14.3
Ba $5s$	27.0	27.8
Br $3d_{5/2}$		66.2
$3d_{3/2}$		67.0
Ba $4d_{5/2}$	87.0	87.8
$4d_{3/2}$	89.6	90.4
$N_{4,5}\text{-O}_{2,3}\text{V}$	71.2	71.4
$N_{4,5}\text{-O}_{2,3}\text{O}_{2,3}$	56	55.4
	58.4	57.8

were measured at an excitation-photon energy of 110 eV, are also shown in Table I with respect to the top of the valence band for convenience. The Auger electron peaks and Ba $5p$ photoelectron peaks are enhanced beyond the threshold of the Ba $4d$ excitation. In order to see the photon-energy dependence of these enhancements in more detail, the constant-final-state (CFS) spectra with the final state corresponding to the kinetic energy of the $N_{4,5}\text{-O}_{2,3}\text{O}_{2,3}$ Auger electron and the constant-initial-state (CIS) spectra with the initial states at the peak of the Ba $5p$ level were observed. The results are shown in Figs. 3 and 4, together with the Ba- $N_{4,5}$ absorption spectra, whose absorption coefficient is given on the right-hand side of the figures.

As seen in Figs. 3 and 4, absorption spectra of BaCl_2 and BaBr_2 show sharp lines *A* and *B* due to the $4d^9 4f^1$ multiplet (3P and 3D) and structures *C* through *H* originating from the $4d^9 4f^1$ 1P states. The other states such as $4d^9 n f^1$ states ($n = 5, 6$, and so on) may mix into the structures. The CFS spectra with the final state at the $N_{4,5}\text{-O}_{2,3}\text{O}_{2,3}$ Auger electron peak and the $5p_{1/2}$ -CIS spectrum (the CIS spectrum with the initial state at the Ba $5p_{1/2}$ level) show sharp lines and structures corresponding to the absorption lines and structures in Ba halides. Strictly speaking, the kinetic energy of the $N_{4,5}\text{-O}_{2,3}\text{O}_{2,3}$ Auger electron shifts due to a two-hole-and-one-electron interaction¹⁴) and the CFS spectra contain the background due to the inelastic scattering of Ba $5p$, Ba $5s$, halogen s , and valence-band photoelectrons. However, the amount of the energy shift is small (less than 1.2

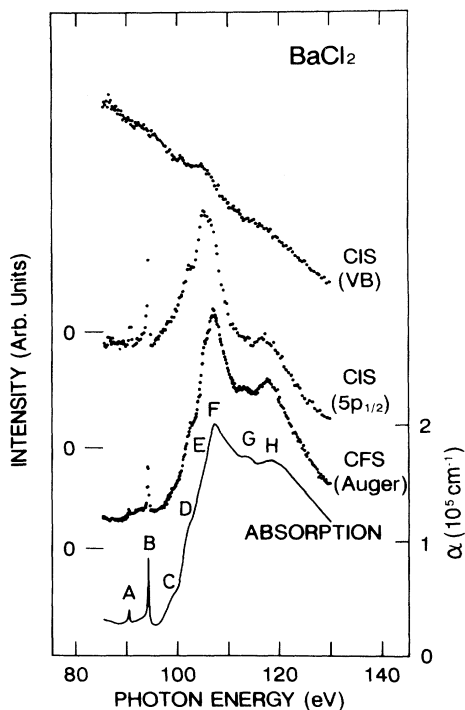


FIG. 3. The valence-band CIS, Ba $5p_{1/2}$ CIS, CFS, and absorption spectra of BaCl_2 . The absorption coefficient is given on the right-hand side of the figure.

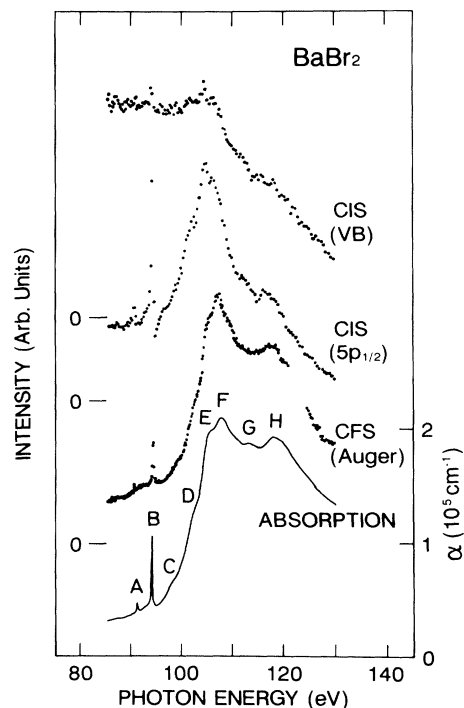


FIG. 4. The valence-band CIS, Ba $5p_{1/2}$ CIS, CFS, and absorption spectra of BaBr_2 . The absorption coefficient is given on the right-hand side of the figure.

eV) relative to the bandwidth of Auger electrons (the full width at half maximum is about 5 eV), and the background due to the inelastic scattered electrons is smooth and small in comparison with the Auger electron intensity, and then these do not change drastically the spectral feature of the observed CFS spectra.

Intensity distributions of the CFS and absorption spectra in BaCl_2 and BaBr_2 are similar to each other, while the intensity distribution of the $5p$ -CIS spectra is much different from that of the absorption spectra. These results are in good agreement with that for BaF_2 reported in Ref. 15. It should be noted that the enhancement of the $5p_{1/2}$ -CIS spectra is remarkable for peak *B*, due to the $4d^9 4f^1$ (3D) state, and the enhancement becomes larger in the order of BaF_2 , BaCl_2 , and BaBr_2 . On the other hand, the valence-band intensity of BaCl_2 decreases with little enhancement for peak *E*, as the photon energy is increased, while that of BaBr_2 shows the enhancement for peaks *B* and *F*. This is in contrast to the valence-band CIS spectrum of BaF_2 , which does not show any enhancement around the Ba $4d$ excitation photon energy.

IV. DISCUSSION

Absorption spectra from $4d$ levels in Xe and Xe-like ions are characterized by huge peaks and weak sharp lines. These structures have been explained within an atomic picture,²⁻¹³ and the huge peaks observed in Ba^{++} ($Z = 56$) and La^{+++} ($Z = 57$) have generally been attributed to a $4d^9 4f^1$ (1P) state autoionized into the continuum, while sharp lines have been considered to be

due to the multiplet structures of $4d^9 4f^1$ states located below the ionization threshold. Previously the present authors^{14,15} investigated the nonradiative decay of the $4d$ excited states in Cs halides, BaF_2 , and LaF_3 , and proposed the following nonradiative decay processes as dominant ones: (1) The $N_{4,5}\text{-O}_{2,3}$ direct-recombination process, where an excited electron and a $4d$ hole recombine, resulting in the excitation of the $5p$ electron. The final-state configuration of this direct recombination process is the same as that of the direct photoexcitation of the $5p$ electron, and thus this process causes the enhancement of the $5p$ -CIS spectrum. (2) The $N_{4,5}\text{-O}_{2,3}\text{O}_{2,3}$ Auger process, where a $4d$ hole and a $5p$ electron recombine with the energy transferring to another $5p$ electron. This Auger decay process creates the $N_{4,5}\text{-O}_{2,3}\text{O}_{2,3}$ Auger electrons.

As seen in Figs. 3 and 4, the $5p$ -CIS and CFS spectra of BaCl_2 and BaBr_2 show enhancements in the energy range of Ba $4d$ excitation, indicating that the above nonradiative decay processes exist in these compounds. It should be noted that the CFS spectra are similar in shape to corresponding absorption spectra. This indicates that $4d$ -excited states in BaCl_2 and BaBr_2 decay dominantly through the $N_{4,5}\text{-O}_{2,3}\text{O}_{2,3}$ process [process (2) mentioned above], and is consistent with the fact that strong Auger peaks are observed in Figs. 1 and 2. This result is the same as in cesium halides, BaF_2 , and LaF_3 (Refs. 14 and 15).

In contrast, the spectral features of the $5p$ -CIS spectra of BaCl_2 and BaBr_2 are much different from those of the absorption spectra. This indicates that the probability of the $4d$ -excited states through the $N_{4,5}\text{-O}_{2,3}$ decay process is not constant over the Ba $N_{4,5}$ excitation region. The decay probability of the $N_{4,5}\text{-O}_{2,3}$ process can be estimated from the $5p$ -CIS and the absorption spectra according to the following formula:

$$P = \frac{\Delta I_{5p}(hv)/I_{5p}(hv)}{\alpha_{4d}(hv)/\alpha_{5p}(hv)}, \quad (1)$$

where ΔI_{5p} and I_{5p} are the incremental enhancement of the Ba $5p$ photoelectron intensity due to the $N_{4,5}\text{-O}_{2,3}$ process and the Ba $5p$ photoelectron intensity without any resonant enhancement, respectively. Also, α_{4d} and α_{5p} are parts of the absorption coefficient due to the formation of $4d$ -excited states and due to the transition from the Ba $5p$ level to the continuum, respectively. The derivation of the formula has been reported in detail elsewhere.¹⁴

The estimated decay probability of peak *B* due to the $4d^9 4f^1$ (3D) state in BaF_2 , BaCl_2 , and BaBr_2 is 1%, 3.5%, and 12%, respectively, while that of peak *E* at 103 eV (the 1P state) is 0.8%, 2%, and 6%, respectively. It is noteworthy that the decay probability of the 3D state is larger than that of the 1P state in all of the barium halides. This is consistent with the idea that the 3D state is well localized below the ionization threshold, while the 1P state above the threshold must be extended to be autoionized.^{2,14}

Figure 5 shows the detailed comparison of the Ba $5p$ photoelectron spectra around the excitation photon ener-

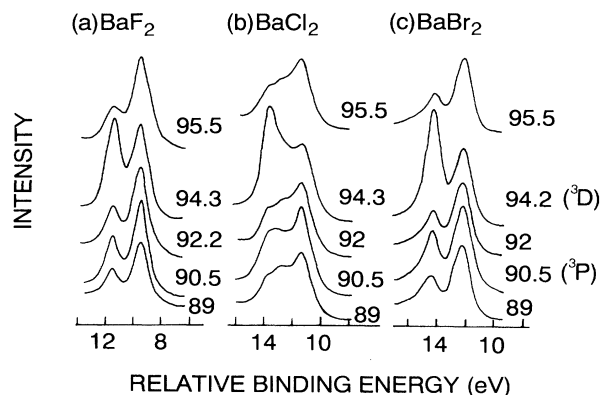


FIG. 5. Detailed comparison of Ba $5p$ photoelectrons around the excitation photon energy of the 3P and 3D states.

gy for 3P and 3D states. The intensity ratio between Ba $5p_{1/2}$ and $5p_{3/2}$ photoelectrons changes remarkably in Ba halides, although the Cl $3s$ photoelectron appears between Ba $5p_{1/2}$ and $5p_{3/2}$ photoelectrons in BaCl_2 . The intensities of Ba $5p_{1/2}$ and $5p_{3/2}$ photoelectrons, which were derived from the set of photoelectron spectra by subtracting the contributions of the background and Cl $3s$ photoelectrons, are shown in Fig. 6. The intensity of the Ba $5p_{1/2}$ photoelectron is normalized at 89 eV in the figure. The contribution of photoelectrons from the Br $4s$ level could not be subtracted, since it is buried under the Ba $5p_{3/2}$ level. As seen in these figures, the intensity ratio of the $5p_{1/2}$ to $5p_{3/2}$ photoelectrons deviates from the statistical weight ($\frac{1}{2}$) at 90.5 and 94.3 eV, which correspond to the excitation photon energy of the 3P and 3D states, respectively. This anomalous intensity ratio can be interpreted in terms of the different branching ratio in nonradiative decay of $4d^9 4f^1$ states into $5p_{1/2}^{-1} 6d^1$ and $5p_{3/2}^{-1} 6d^1$ states. Recently, Ogasawara *et al.*¹⁷ have succeeded in explaining the anomalous intensity ratio between La $5p_{1/2}$ and $5p_{3/2}$ photoelectrons in LaF_3 by taking account of the multiplet dependence of the transition probabilities for the direct-recombination process. Their calculation agrees qualitatively with the present results for Ba halides.

Previously, Miyahara *et al.*¹⁰ found the difference in the giant Ba $4d$ absorption structures between metallic

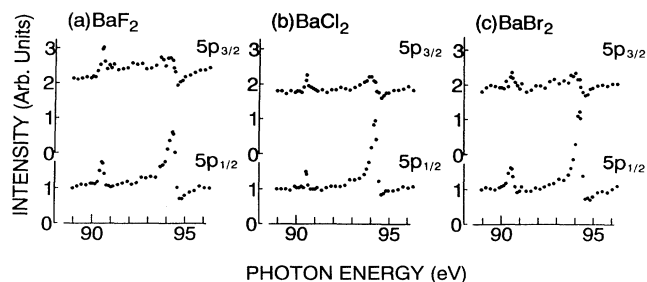


FIG. 6. Detailed comparison of Ba $5p_{3/2}$ and $5p_{1/2}$ photoelectron intensities derived from a set of photoelectron spectra. The Ba $5p_{1/2}$ intensity obtained with 89 eV is normalized.

Ba and BaF₂, and between amorphous and crystalline BaF₂. They suggested that the amount of hybridization of 5*f* or 6*f* states with the 4*d*⁹4*f*¹ ¹P state or continuum states are dependent on the crystal structure. As mentioned above, the nonradiative decay probability of ³D and ¹P states through the N_{4,5}-O_{2,3} process increases in the order of BaF₂, BaCl₂, and BaBr₂. This result shows that the solid-state effects occur for the ³D state below the 4*d* threshold as well as the ¹P state autoionized into the continuum. Moreover, as shown in Fig. 6, the anomalous intensity ratio of 5*p*_{1/2} to 5*p*_{3/2} photoelectrons becomes larger in the order from BaF₂ to BaBr₂. As mentioned above, the calculation by Ogasawara *et al.*¹⁷ agrees qualitatively with the observed anomalous intensity ratio. Although their calculation cannot explain the observed difference in the intensity ratio among barium halides since their calculation is limited within an atomic picture, the matrix elements for direct recombination decay depend on the radial integrals of 4*d*⁹4*f*¹ and 5*p*⁵*ed*¹ states. Thus we suggest that the spatial distribution as well as the nonradiative decay probability of 4*d*⁹4*f*¹ states are affected not only by the atomic-wave-function collapse due to a 4*d* hole, but also by the crystalline field in barium halides.

As seen in Figs. 3 and 4, and Fig. 4 in Ref. 15, the N_{4,5}-V decay process, where a 4*d* hole and an excited electron recombine with the energy being transferred to valence electrons, is not appreciable in BaF₂, but is weakly observed in BaCl₂ and clearly seen in BaBr₂. The decay probability of the ³D state (the peak *B*) through the N_{4,5}-V process in BaF₂, BaCl₂, and BaBr₂ is 0%, 0%, and 1.3%, respectively, while that of peak *E* is 0%, 1%, and 2%, respectively. This shows that the mixing of the barium and halogen wave functions in the valence band becomes larger in the order from BaF₂ to BaBr₂. This is consistent with the fact that the ionicity of the halogen ion is in the order from Br⁻ to F⁻. As mentioned above, the decay probability of ¹P through the N_{4,5}-O_{2,3} process is smaller than that of ³D in barium halides. This is consistent with the above idea based on the wave-function mixing between barium and halogen ions, since the ¹P state spreads spatially more than the ³D state, resulting in the wave-function mixing. The anomalous increase in the branching ratio between 5*p*_{1/2} and 5*p*_{3/2} photoelectrons is also consistent with this idea, since the mixing of barium and halogen wave functions may change the matrix elements for direct recombination decay through the N_{4,5}-O_{2,3} process, resulting in an increase in the intensity ratio of 5*p*_{1/2} to 5*p*_{3/2} photoelectrons.

On the other hand, the fact that the decay probability of the N_{4,5}-O_{2,3} process increases in the order of BaF₂,

BaCl₂, and BaBr₂ is not easily understood in terms of the mixing of barium and halogen wave functions. One might imagine that, as the mixing is increased from BaF₂ to BaBr₂, the 4*d*⁹4*f*¹ states become delocalized, to result in the decrease in the N_{4,5}-O_{2,3} decay process. This is not the case. Then we suggest that if the mixing of the wave functions decreases the N_{4,5}-O_{2,3}O_{2,3} process more than the N_{4,5}-O_{2,3} process, the decay probability of the N_{4,5}-O_{2,3} process may increase as the present experimental result. This is because the decay probability is determined by the competition between various decay processes. In fact, the ratio of the integrated intensity of the N_{4,5}-O_{2,3}O_{2,3} Auger electron peak to the incremental enhancement of Ba 5*p* photoelectrons (ΔI_{5p}) decreases in going from BaF₂ to BaBr₂ (see Figs. 1 and 2, and Fig. 3 in Ref. 15). Further theoretical studies, however, are needed to confirm the present suggestion.

In conclusion, the nonradiative decay of 4*d*⁹4*f*¹ states in Ba halides was investigated by using resonant photoemission spectroscopy with synchrotron radiation. It was found that the CFS spectra agree in shape with the absorption spectra, indicating that the 4*d*⁹4*f*¹ states decay dominantly through the Auger process. On the other hand, the CIS spectra with the initial states at the Ba 5*p* level and the valence band were also found to be enhanced around the Ba N_{4,5} excitation energy region, indicating the decay processes through a direct recombination between a 4*d* hole and an excited electron. Spectral features of the 5*p*-CIS spectra did not coincide with those of the absorption spectra. The intensity ratio of 5*p*_{1/2} to 5*p*_{3/2} photoelectrons showed the anomalous increase for the ³D state. Moreover, the probability through the direct recombination process and the degree of the anomalous branching ratio showed the increase in the order from BaF₂ to BaBr₂. From these results, we suggested that the localization of 4*d*⁹4*f*¹ states is not constant over the Ba N_{4,5} excitation energy region, and that the spatial distribution as well as the nonradiative decay probability of 4*d*⁹4*f*¹ states are affected by the crystalline field, as well as the atomic-function collapse due to a 4*d* hole.

ACKNOWLEDGMENTS

The authors would like to express their sincere thanks to the staffs of the INS-SOR facility of the University of Tokyo, and members of the UVSOR facility of the Institute of Molecular Science, who helped them conduct photoelectron and absorption experiments. They also thank Professor A. Kotani of the University of Tokyo for discussions.

¹See, for example, *Handbook of the Physics and Chemistry of the Rare Earths*, edited by K. A. Gschneidner, Jr. and L. Eyring (North-Holland, Amsterdam, 1978), and references therein.

²J. Sugar, *Phys. Rev. B* **5**, 1785 (1972).

³G. Wendin, in *Vacuum Ultraviolet Radiation Physics*, edited by E. E. Koch, R. Haensel, and C. Kunz (Pergamon Vieweg, Hamburg, 1974), p. 225.

⁴M. Ya, Amusia, V. K. Ivanov, and L. V. Chernysheva, *Phys.*

Lett. **29**, 191 (1976).

⁵J. P. Connerade, *Contemp. Phys.* **19**, 415 (1978).

⁶R. I. Karaziya, *Usp. Fiz. Nauk* **135**, 79 (1981) [*Sov. Phys. Usp.* **24**, 775 (1981)].

⁷T. B. Lucatorto, T. J. McIlrath, J. Sugar, and S. M. Younger, *Phys. Rev. Lett.* **47**, 1124 (1981).

⁸J. P. Connerade and M. W. D. Mansfield, *Phys. Rev. Lett.* **48**, 131 (1982).

- ⁹K. T. Cheng and C. F. Fischer, *Phys. Rev. A* **28**, 2811 (1983).
- ¹⁰T. Miyahara, T. Hanyu, H. Ishii, M. Yanagihara, T. Kamada, H. Kato, K. Naito, and S. Suzuki, *J. Phys. Soc. Jpn.* **55**, 408 (1986).
- ¹¹O. Aita, K. Ichikawa, M. Kamada, M. Okusawa, H. Nakamura, and K. Tsutsumi, *J. Phys. Soc. Jpn.* **56**, 649 (1987).
- ¹²M. Ya. Amusia, L. V. Chernysheva, V. K. Ivanov, and V. A. Kupchenko, *Z. Phys. D* **14**, 215 (1989).
- ¹³T. Jo, *J. Phys. Soc. Jpn.* **58**, 1452 (1989).
- ¹⁴M. Kamada, O. Aita, K. Ichikawa, M. Okusawa, and K. Tsutsumi, *Phys. Rev. B* **45**, 12 725 (1992).
- ¹⁵K. Ichikawa, O. Aita, K. Aoki, M. Kamada, and K. Tsutsumi, *Phys. Rev. B* **45**, 3221 (1992).
- ¹⁶K. Ichikawa, M. Kamada, O. Aita, and K. Tsutsumi, *Phys. Rev. B* **32**, 8293 (1985).
- ¹⁷H. Ogasawara, A. Kotani, B. T. Thole, K. Ichikawa, O. Aita, and M. Kamada, *Solid State Commun.* **81**, 645 (1992).